

## Blooms of the harmful algae *Margalefidinium polykrikoides* and *Alexandrium monilatum* alter the York River Estuary microbiome

Samantha G. Fortin <sup>a,\*</sup>, Bongkeun Song <sup>a,\*</sup>, Iris C. Anderson <sup>a</sup>, Kimberly S. Reece <sup>a</sup>

<sup>a</sup> Virginia Institute of Marine Science, William and Mary, Gloucester Point, VA, USA

### ARTICLE INFO

Editor: Dr. C. Gobler

**Keywords:**

*Alexandrium monilatum*  
*Margalefidinium polykrikoides*  
Microbiome  
Harmful dinoflagellate bloom

### ABSTRACT

Harmful algal blooms (HABs) cause damage to fisheries, aquaculture, and human health around the globe. However, the impact of HABs on water column microbiomes and biogeochemistry is poorly understood. This study examined the impacts of consecutive blooms of the ichthyotoxic dinoflagellates *Margalefidinium polykrikoides* and *Alexandrium monilatum* on the water microbiome in the York River Estuary, Chesapeake Bay, USA. The samples dominated by single dinoflagellate species and by a mix of the two dinoflagellates had different microbiome compositions than the ones with low levels of both species. The *M. polykrikoides* bloom was co-dominated by *Winogradskya* and had increased concentrations of dissolved organic carbon. The *A. monilatum* bloom had little impact on the prokaryotic portion of the whole community but was associated with a specific group of prokaryotes in the particle-attached ( $>3 \mu\text{m}$ ) fraction including *Candidatus Nitrosopumilus*, *Candidatus Actinomarina*, SAR11 Clade Ia, *Candidatus Bealeia*, and *Rhodobacteraceae* HIMB11. Thus, blooms of these two algal species impacted the estuarine microbiome in different ways, likely leading to shifts in estuarine carbon and nutrient cycling, with *M. polykrikoides* potentially having a greater impact on carbon cycling in the estuarine ecosystem than *A. monilatum*.

### 1. Introduction

Harmful algal blooms (HABs), blooms of algae that produce toxins or harm the aquatic environment, are increasing in number and impact worldwide (Heisler et al., 2008; Sellner et al., 2003). Some HABs pose a public health risk by inducing paralytic, amnesiac, diarrheic, or neuro-toxic shellfish poisoning in people consuming shellfish containing HAB toxins. HABs are also of economic concern as they can lead to mass fish and shellfish mortality or the closure of industry operations due to human health risks, negatively impacting aquaculture and commercial fisheries (Kudela and Gobler, 2012). Despite our growing knowledge of the ecology and causes of harmful algal blooms, which include eutrophication and nutrient loading (Heisler et al., 2008; Sellner et al., 2003), more studies are needed to gain a better understanding of bloom formation, the environmental controls on specific algal species, and how harmful algal blooms impact other estuarine microorganisms.

Currently, the impact of harmful algal blooms on the microbiome, defined here as the overall community of prokaryotes and microbial eukaryotes, of estuaries and rivers is not well understood and has only been investigated for a small subset of harmful algal species and

locations. Many free-living, attached, and intracellular prokaryotes associated with algae, both harmful and non-harmful, are essential to algal physiology and growth (Buchan et al., 2014; Croft et al., 2005; Kodama et al., 2006) and aquatic prokaryotes and microbial eukaryotes are impacted by large blooms of any phytoplankton (Azam et al., 1983), including those classified as harmful algae (Hattenrath-Lehmann et al., 2019; Hattenrath-Lehmann and Gobler, 2017; Koch et al., 2014). In general, algal blooms are hotspots of primary production and produce large amounts of organic matter, encouraging the growth of heterotrophic microbes and the remineralization of that organic matter, leading to changes in carbon and nutrient biogeochemistry (Azam et al., 1983; Buchan et al., 2014). HABs are no exception to this rule, but also have additional interactions with prokaryotic species. Various prokaryotic species have been found to produce algicidal compounds that impact HABs and in some cases prokaryotes have been found to aid in the production of phycotoxins or to produce HAB associated toxins themselves (Doucette, 1995). Additionally, many harmful algae, including dinoflagellates, are mixotrophic, allowing them to consume prokaryotes or other microbial eukaryotes as food sources (Jeong et al., 2010; Stoecker et al., 2017).

\* Corresponding authors.

E-mail addresses: [sgfortin@vims.edu](mailto:sgfortin@vims.edu) (S.G. Fortin), [songb@vims.edu](mailto:songb@vims.edu) (B. Song).

Phytoplankton blooms are common throughout many estuaries across the globe, including in the Chesapeake Bay, USA. The York River Estuary, the 5th largest tributary to Chesapeake Bay (Reay, 2009), experiences near annual summer blooms of HAB species in the lower portion of the estuary (Marshall and Egerton, 2009; Reay, 2009). For more than 50 years, the summer blooms were dominated by the ichthyotoxic dinoflagellate *Margalefidinium polykrikoides* (Gómez et al., 2017), formerly classified as *Cochlodinium polykrikoides* (Marshall and Egerton, 2009). In 2007, a second toxic dinoflagellate *Alexandrium monilatum* (Howell) (Balech, 1995), began to bloom after the decline of the *M. polykrikoides* bloom, setting up a near-annual cycle of two consecutive HABs in the late summer and early fall (Marshall and Egerton, 2009). Both HAB species are thought to be mixotrophic and have been associated with fish and shellfish kills in the Chesapeake Bay and elsewhere (Anderson et al., 2012; Harding et al., 2009; Kudela and Gobler, 2012; May et al., 2010; Mulholland et al., 2009).

*Margalefidinium polykrikoides* has been studied extensively off the coast of South Korea where it has devastated fisheries and aquaculture for decades due to its negative impact on the health of larval fish and shellfish (Kudela and Gobler, 2012; Lee et al., 2013; Tang and Gobler, 2009), though the North American variants present on the East Coast of the United States, including in the Chesapeake Bay, have not been as well studied (Gobler et al., 2012; Mulholland et al., 2009). Previous studies examining the impact of *M. polykrikoides* blooms on water column microbiomes have determined that *M. polykrikoides* bloom communities are dominated by taxa belonging to the orders *Gammaproteobacteria*, *Rhodobacteriales*, and *Flavobacteriales*, with one study in a New York estuary finding that species belonging to the genera *Winogradskyella* (*Flavobacteriales*) and *Coraliomargarita* (*Opitutales*) were highly abundant members of bloom microbiomes (Hattenrath-Lehmann et al., 2019; Koch et al., 2014; Shin et al., 2018).

*Alexandrium monilatum*, a thecate dinoflagellate which produces the toxin gonydmin A, forms blooms in the Chesapeake Bay and along the Florida and Gulf of Mexico coasts leading to fish and shellfish mortalities (España et al., 2016; Hsia et al., 2006; Marshall and Egerton, 2009); however, it is not as widely studied as other toxic *Alexandrium* species like *A. tamarense* and *A. catenella* which produce saxitoxins. In fact, the bacterial assemblage associated with blooms of *A. monilatum* has not previously been examined. Previous studies on blooms dominated by members of the genus *Alexandrium*, including *A. fundyense* (now synonymized with *A. catenella*) and *A. tamarense*, have found the prokaryotic communities of *Alexandrium* blooms to be dominated by taxa in the orders *Flavobacteriales*, *Rhodobacteriales*, and the SAR11 Clade (Hattenrath-Lehmann and Gobler, 2017; Jasti et al., 2005; Shin et al., 2018). One study on an *A. fundyense* bloom found the dominant prokaryotic genera to be the NS5 marine group (*Flavobacteriales*), an uncultured *Rhodobacteriales*, and *Owenweeksia* (*Flavobacteriales*) (Hattenrath-Lehmann and Gobler, 2017).

Despite the previous research examining changes in microbiomes associated with blooms, few studies have examined consecutive blooms in the same location (Hattenrath-Lehmann and Gobler, 2017) and only a few microbiome studies have taken advantage of the large amount of data provided by advanced metabarcoding sequencing techniques (Garcés et al., 2007). Furthermore, past studies have not examined the impact of changes in specific biogeochemical variables associated with blooms on the microbiome. To address these remaining questions, we examined a consecutive HAB event in the York River Estuary, starting with 1) a mixed bloom of *M. polykrikoides* and *A. monilatum*, 2) a bloom of *M. polykrikoides*, 3) a transition period between blooms of the two species, and 4) a bloom of *A. monilatum*. In addition, we compared the whole community to the particle-attached fraction of the microbiome in water samples collected from patches with high concentrations or very low or no concentration of the HAB species. We identified prokaryotic taxa that are associated with the HAB species in the particle-attached fraction and determined correlations between the abundances of prokaryotic and microbial eukaryotic taxa and the biogeochemical features

associated with the HAB events in the York River Estuary.

## 2. Methods

### 2.1. Field sampling

The York River Estuary receives the majority of its nutrients through runoff from forested and agricultural land and a smaller proportion from wastewater treatment plants (Reay, 2009). The lower portion of the estuary experiences blooms most years, many of which involve HAB species (Reay, 2009). Water samples were collected four times between August 1, 2017 and August 22, 2017 during the period of HAB events in the lower York River Estuary (Fig. 1). During each sampling period, surface water samples were taken for microbiome analysis, phytoplankton cell counts, and nutrient analyses at 6 locations: 3 replicate in-bloom patches characterized by increased in situ chlorophyll levels and discoloration of the water and 3 replicate out-of-bloom patches characterized by lower in situ chlorophyll levels and a lack of discoloration in the water. In- and out-of-bloom patches were later confirmed based on *M. polykrikoides* and *A. monilatum* cell counts from qPCR with an average of 1000 cells mL<sup>-1</sup> considered an in-bloom patch. YSI readings were taken at each station to record salinity, temperature, in situ chlorophyll levels, dissolved oxygen (DO) concentrations, and turbidity.

Surface water samples for whole microbiome analysis were filtered immediately through 0.22 µm Sterivex filters until 300 mL of water were filtered or the filter clogged, whichever came first. The filters were then frozen on dry ice, brought back to the lab, and stored at -80 °C until processed. Additional water samples were taken in three 120 mL sterile bottles and were brought back to the lab where 50–100 mL of the sample, depending on the concentration of chlorophyll noted in the field, were filtered onto 3 µm Isopore™ membrane filters (Millipore Corp., Darmstadt, Germany) to examine the microbiomes attached to phytoplankton and particles > 3 µm in size. The filters were stored at -20 °C until processed. Samples for nutrient analysis, including dissolved nitrate/nitrite (NO<sub>x</sub>), dissolved ammonium (NH<sub>4</sub><sup>+</sup>), dissolved organic nitrogen (DON), and dissolved organic carbon (DOC) were brought back to the lab and frozen until analysis after filtration through 0.45 µm polyethersulfone (PES) cartridge filters. Ammonium and NO<sub>x</sub> concentrations were measured in duplicate using a Lachat QuikChem FIA+ 8000 (detection limits: 0.2 µM nitrate and nitrite, 0.36 µM ammonium) (Liao, 2001; Smith and Bogren, 2001). DON was also run on the Lachat after combustion using a persulfate reduction method (Koroleff, 1983). DOC samples were analyzed using a Shimadzu TOC-Vcsn analyzer (Sharp et al., 2004). Samples for dissolved inorganic carbon (DIC) were placed in Exetainer tubes and spiked with a 10x dilution of saturated mercuric chloride solution in the field; all DIC samples were run on an Apollo SciTech AS-C3 DIC analyzer mated with a Licor LI-7000 CO<sub>2</sub>/H<sub>2</sub>O analyzer (Neubauer and Anderson, 2003). Samples for active chlorophyll were collected in the field and filtered on GF/F filters before being frozen prior to analysis; chlorophyll was extracted with a DMSO/acetone solution and run on a Turner 10-AU fluorometer (Anderson et al., 2003).

### 2.2. Microbiome analysis

DNA was extracted from the 0.22 µm and 3 µm filters using the QIAamp DNA Stool Kit (Qiagen) following the manufacturer's protocol modified to increase cell lysis with a 95 °C incubation step and the use of an additional 50 µL of Proteinase K. Extracted DNA from both filters was amplified using the primers 515F-Y and 926R (Parada et al., 2016), which are designed to amplify both 16S and 18S rRNA gene fragments, allowing both prokaryotic and eukaryotic microbes in the collected samples to be examined. The PCR program included a 95 °C step for 3 min followed by 30 cycles of 95 °C for 30 s, 55 °C for 1 min and 72 °C for 1 min with a final 5 min step at 72 °C. All PCR reactions consisted of 12.5

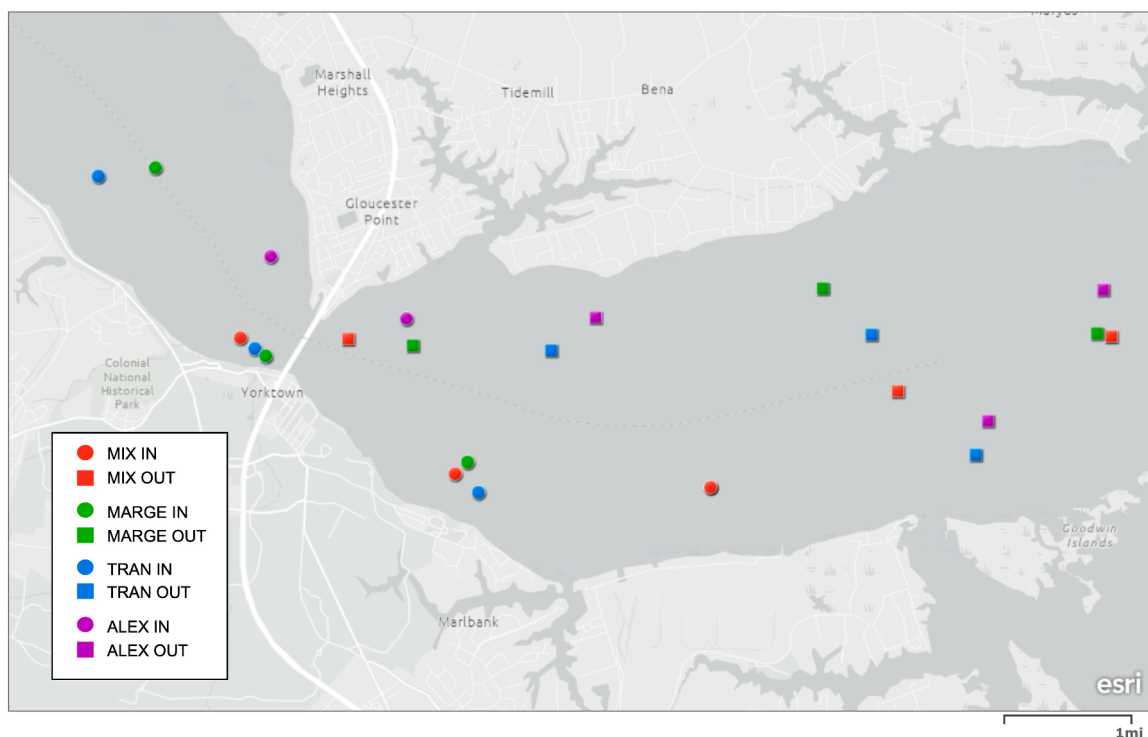


**Fig. 1.** A map of sampling stations in the lower York River during the 2017 harmful algal bloom cycle. In-bloom (circle) and out-of-bloom (square) patches are designated by shape; bloom conditions, mix of *M. polykrikoides* and *A. monilatum* (MIX, red), *M. polykrikoides* dominated bloom (MARG, green), transition between blooms (TRAN, blue), and *A. monilatum* dominated bloom (ALEX, purple), are represented by different colors. One ALEX in-bloom station was located at the same location as a MIX in-bloom station and is hidden from view on the map.

$\mu$ L of GoTaq Master Mix (Promega), 1  $\mu$ L of each primer (10 mM), and 1 ng of DNA with the rest of the 25  $\mu$ L solution made up of water. Amplified genes were indexed using a Nextera XT index primer kit and cleaned using a Mag-Bind Total Pure NGS Kit (Omega Bio-Tek) following manufacturer protocols before being sequenced on an Illumina MiSeq. All sequences can be found in the NCBI GenBank under BioProject number PRJNA731462.

The cell numbers of the targeted HAB species present in the samples were determined with TaqMan quantitative PCR (qPCR) assays using DNA extracted from the 3  $\mu$ m filters following the protocols described in Vandersea et al. (2017) and Wolny et al. (2020) for *A. monilatum* and *M. polykrikoides*, respectively. Samples were run in triplicate and gene concentrations were calculated based on standard curves extracted from samples with known cell counts obtained from in vitro cultures assumed to be growing asexually that are maintained at the Virginia Institute of Marine Science (VIMS). Since qPCR assays measure gene counts, and since the number of target genes per genome is not currently known for *M. polykrikoides* or *A. monilatum*, the qPCR results are calculated as counts per genome. The standards used to calculate qPCR genome copy numbers have one genome per cell, so the number of genomes  $\text{mL}^{-1}$  can be used as an equivalent to the number of cells  $\text{mL}^{-1}$ .

All bioinformatic and statistical analyses were performed using R version 4.0.3 (R Core Team, 2018) and figures were made using ggplot2 (Wickham, 2009). Microbial rRNA sequences, excluding chloroplast and mitochondrial sequences, that passed quality control and chimera checks were trimmed and identified using SILVA version 132 (Yilmaz et al., 2014) and the DADA2 package (Callahan et al., 2016). Amplicon sequence variants (ASVs) obtained from DADA2 that were not present in at least three samples, representing the three replicate samples from each patch and bloom condition, were not included in the analysis. Microbial community data were analyzed using the phyloseq package (McMurdie and Holmes, 2013) including principal component analyses (PCoA) and heatmap analyses. Replicates were combined for the heatmap analysis using the phylosmith package (Smith, 2019).

Permutational multivariate analysis of variance (PERMANOVA) tests were run on data that was homogeneously dispersed, based on the betadispr function in the vegan package (Oksanen et al., 2018), using the adonis function in vegan and a Bray-Curtis distance matrix calculated with phyloseq to compare variation in microbiome structure across different patch and bloom conditions. Spearman correlations between the relative abundance of taxa and concentrations of  $\text{NO}_x$ ,  $\text{NH}_4^+$ , DON, DIC, and DOC were calculated using the microbiomeSeq package (Ssekagiri et al., 2017) with p-values adjusted for multiple comparisons following the Benjamin and Hochberg method; correlations were considered significant with an adjusted p-value  $< 0.05$ .

### 3. Results

#### 3.1. Bloom environmental conditions

Samples from in-bloom patches and out-of-bloom patches were collected during the 2017 HAB cycle in the lower portion of the York River (Figure 1). During the first week of the bloom cycle, cells of both harmful algal species, *Margalefidinium polykrikoides* and *Alexandrium monilatum*, were present in the system. During this week, the in-bloom average of *M. polykrikoides* was 13,177 ( $\pm 5514$ , standard error) and of *A. monilatum* was 1518 ( $\pm 897$ ) cells  $\text{mL}^{-1}$ , while the out-of-bloom samples had less than 30 cells  $\text{mL}^{-1}$  of either species (Table 1). This first bloom week was designated as a mixed bloom (MIX) due to the presence of both species at a concentration above bloom levels ( $> 1000$  cells  $\text{mL}^{-1}$  in in-bloom patches on average). The second week of the bloom cycle was dominated by *M. polykrikoides* with in-bloom cell counts averaging 37,200 ( $\pm 6604$ ) while *A. monilatum* cell counts were an average of 89 ( $\pm 17$ ) in the in-bloom samples; this week was designated as an *M. polykrikoides* bloom (MARG) due to the high cell counts of *M. polykrikoides*. In the third week of the bloom cycle, *M. polykrikoides* was on average 1 cell  $\text{mL}^{-1}$  and *A. monilatum* was on average 1060 ( $\pm 541$ ) cells  $\text{mL}^{-1}$  in in-bloom samples; this week was designated a

**Table 1**

Environmental characteristics of surface water collected in and out of harmful algal bloom patches in August 2017 in the York River. Bloom describes the bloom condition (MIX: mix of *M. polykrikoides* and *A. monilatum*; MARG: bloom dominated by *M. polykrikoides*; TRAN: transition between blooms; ALEX: bloom dominated by *A. monilatum*) at the time of collection. Patch refers to in-bloom (IN) versus out-of-bloom (OUT) samples. All variables are averages of three replicates (standard error) including: a count of *Margalefidiinium polykrikoides* cells determined by qPCR (Marge Count), a count of *Alexandrium monilatum* cells determined by qPCR (Alex Count), active chlorophyll *a* extracted from filtered water (Active chl *a*), water temperature (Temp), dissolved inorganic nitrogen concentrations including nitrate/nitrite ( $\text{NO}_x$ ) and ammonium ( $\text{NH}_4^+$ ), dissolved organic nitrogen (DON), dissolved inorganic carbon (DIC), and dissolved organic carbon (DOC).

Date	Bloom	Patch	Marge count (cells/mL)	Alex count (cells/mL)	Active chl <i>a</i> ( $\mu\text{g/L}$ )	Temp ( $^{\circ}\text{C}$ )	Salinity	$\text{NO}_x$ ( $\mu\text{M}$ )	$\text{NH}_4^+$ ( $\mu\text{M}$ )	DON ( $\mu\text{M}$ )	DIC (mM)	DOC ( $\mu\text{M}$ )
8/1/17	MIX	IN	13,177 (5514)	1518 (897)	109.6 (39.8)	27.4 (0.3)	22.1 (0.1)	1.1 (0.7)	1.3 (0.7)	85.2 (36.5)	1.3 (0.1)	1182.7 (427.6)
8/1/17	MIX	OUT	22 (11)	15 (1)	10.4 (2.5)	27.3 (0.2)	22.2 (0.0)	0.3 (0.0)	0.3 (0.0)	16.4 (0.1)	1.6 (1.0)	231.5 (9.0)
8/9/17	MARG	IN	37,200 (6604)	89 (17)	247.9 (27.0)	26.9 (0.2)	21.6 (0.1)	0.3 (0.0)	0.3 (0.0)	46.2 (0.1)	1.6 (5.0)	750.9 (62.2)
8/9/17	MARG	OUT	1 (0)	10 (8)	9.0 (1.7)	26.2 (0.2)	21.2 (0.2)	0.3 (0.0)	0.1 (0.0)	23.2 (0.1)	1.7 (0.7)	317.5 (8.3)
8/16/17	TRAN	IN	1 (0)	1060 (541)	20.7 (5.7)	27.6 (0.2)	21.1 (0.1)	2.9 (0.4)	1.7 (0.6)	25.2 (0.6)	1.6 (0.9)	360.9 (2.8)
8/16/17	TRAN	OUT	1 (0)	1 (1)	6.8 (0.2)	27.7 (0.1)	20.7 (0.1)	0.6 (0.1)	0.2 (0.1)	22.4 (0.0)	1.6 (0.1)	302.4 (27.7)
8/22/17	ALEX	IN	1 (0)	58,105 (22,143)	171.7 (17.6)	29.0 (0.2)	20.7 (0.1)	1.1 (0.3)	0.4 (0.0)	29.8 (3.5)	1.5 (0.0)	419.1 (36.3)
8/22/17	ALEX	OUT	0 (0)	181 (166)	10.7 (2.5)	28.4 (0.3)	20.4 (0.1)	0.7 (0.2)	0.3 (0.0)	22.1 (0.0)	1.6 (1.6)	317.0 (40.0)

transition week (TRAN) as the HAB was transitioning from an *M. polykrikoides* dominated to an *A. monilatum* dominated bloom. By the fourth sampling period, *A. monilatum* was on average 58,105 ( $\pm 22,143$ ) cells  $\text{mL}^{-1}$  in the in-bloom samples (Table 1) and, as such, was designated as an *A. monilatum* bloom (ALEX). Relative abundances of *M. polykrikoides* and *A. monilatum*, based on 18S sequencing in the particle-attached fraction, had positive, significant linear relationships with the qPCR-based cell counts (Supplemental Figure 1).

Temperature and salinity remained consistent at in- and out-of-bloom patches for each bloom condition and varied little across the entire bloom cycle in the lower York River (Table 1). Active chlorophyll was higher in in-bloom patches than in out-of-bloom patches for every week of the bloom cycle, though to a lesser degree in TRAN. The highest active chlorophyll was found during MARG (Table 1). The concentrations of  $\text{NO}_x$ ,  $\text{NH}_4^+$ , and DON were generally lower in out-of-bloom patches, though to a small degree in most weeks (Table 1). The concentrations of  $\text{NO}_x$  and  $\text{NH}_4^+$  were highest in TRAN in the in-bloom samples, and DON concentrations were highest in MIX in-bloom samples, followed by the MARG in-bloom samples (Table 1). DIC concentrations were fairly consistent across sampling periods, with the exception of the in-bloom MIX samples; in all weeks but TRAN, DIC concentrations were slightly lower in the in-bloom samples (Table 1). DOC concentrations were higher in in-bloom samples than in out-of-bloom samples, especially during MIX and MARG (Table 1).

### 3.2. Changes in the estuarine microbiome

Sequencing was performed on 16S and 18S rRNA gene fragments

amplified from DNA on the 0.22  $\mu\text{m}$  and 3  $\mu\text{m}$  filters; the DNA extracted from the 0.22  $\mu\text{m}$  filters was used to examine the whole microbiome while the 3  $\mu\text{m}$  filter was used to examine the particle-attached fraction which included the algae, any particles ( $> 3 \mu\text{m}$ ) in the system, and the prokaryotes attached to the algae or any other particles. Alpha diversity in the whole community was lower in in-bloom samples compared to out-of-bloom samples for all weeks except for TRAN where there was no difference in alpha diversity (Table 2).

Beta diversity of the microbiome changed depending on both bloom condition (MIX, MARG, TRAN, or ALEX) and patch (in-bloom or out-of-bloom samples) (Fig. 2). Patterns were the same in the whole community and the particle-attached fraction when considering prokaryotes and eukaryotes together. All out-of-bloom samples clustered with the TRAN in-bloom samples while in-bloom samples from MIX, MARG, and ALEX separated out from the out-of-bloom cluster and from each other (Fig. 2A & 2C). In-bloom samples from MIX, which contained both *M. polykrikoides* and *A. monilatum*, fell between the clustered in-bloom samples from MARG and ALEX (Fig. 2A & 2C). A PERMANOVA test ( $F = 2.3133$ ,  $p = 0.004$ ) confirmed that bloom condition (MIX, MARG, ALEX, and TRAN) was a significant factor driving the difference in prokaryotic and eukaryotic beta diversity in the whole community; however, the effect of patch (in-bloom vs. out-of-bloom) on the whole community could not be tested using a PERMANOVA, nor could the effect of factors on prokaryotic and eukaryotic beta diversity in the particle-attached fraction, due to a lack of homogeneously dispersed data.

When only the prokaryotic members of the microbiome were considered, the patterns in beta diversity differed between the whole

**Table 2**

Alpha diversity indices describing evenness and richness of the whole microbial communities (0.22  $\mu\text{m}$  filter) during each bloom condition (MIX: mix of *M. polykrikoides* and *A. monilatum*; MARG: bloom dominated by *M. polykrikoides*; TRAN: transition between blooms; ALEX: bloom dominated by *A. monilatum*) that occurred in the York River in August 2017. Patch refers to in-bloom (IN) versus out-of-bloom (OUT) patches. All values are averages of three replicates (standard error).

Date	Bloom	Patch	Chao1	ACE	Shannon diversity index	Inverse simpson index
8/1/17	MIX	IN	159.1 (47.9)	160.1 (48.9)	3.0 (0.3)	7.0 (1.3)
8/1/17	MIX	OUT	243.1 (49.3)	244.3 (51.8)	3.8 (0.1)	15.3 (0.8)
8/9/17	MARG	IN	150.8 (25.4)	151.1 (25.5)	3.7 (0.2)	18.3 (2.4)
8/9/17	MARG	OUT	217.4 (6.1)	217.0 (7.6)	4.1 (0.0)	24.1 (0.6)
8/16/17	TRAN	IN	353.4 (157.1)	347.9 (150.3)	4.2 (0.2)	24.9 (1.2)
8/16/17	TRAN	OUT	301.7 (49.5)	303.5 (51.9)	4.1 (0.1)	22.8 (0.5)
8/22/17	ALEX	IN	179.9 (12.7)	176.7 (14.9)	3.0 (0.2)	6.5 (1.4)
8/22/17	ALEX	OUT	269.7 (46.4)	267.9 (43.4)	4.1 (0.1)	22.2 (2.7)

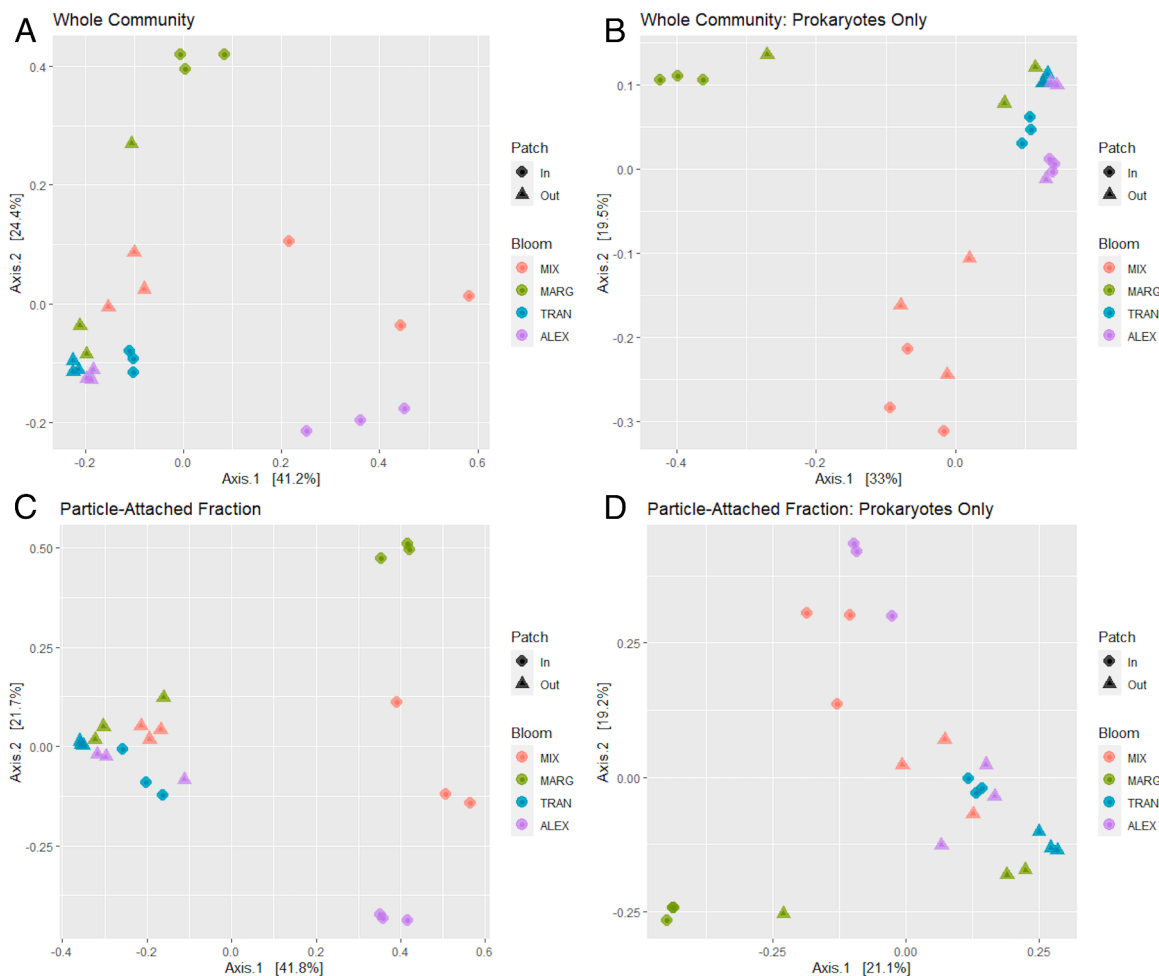


**Fig. 2.** Principal component analysis showing all samples collected during the 2017 harmful algal bloom cycle including (A) the whole community (0.22  $\mu\text{m}$  filter) including prokaryotes and eukaryotes, (B) the whole community (0.22  $\mu\text{m}$  filter) including only prokaryotes, (C) the particle-attached fraction ( $>3 \mu\text{m}$ ) including prokaryotes and eukaryotes, and (D) the particle-attached fraction ( $>3 \mu\text{m}$ ) including only prokaryotes. In-bloom (In) and out-of-bloom (Out) patches are designated by shape; bloom conditions, mix of *M. polykrikoides* and *A. monilatum* (MIX), *M. polykrikoides* dominated bloom (MARG), transition between blooms (TRAN), and *A. monilatum* dominated bloom (ALEX), are represented by different colors.

community and the particle-attached fraction (Fig. 2B & 2D). In the whole community, there were three distinct clusters. MARG in-bloom samples, and one out-of-bloom sample, formed one cluster; the second cluster contained all MIX (in- and out-of-bloom) samples, and the last cluster contained all samples from ALEX and TRAN bloom weeks along with two of the MARG out-of-bloom samples (Fig. 2B). A PERMANOVA test comparing bloom conditions (MIX, MARG, ALEX, TRAN) and patch (in-bloom vs. out-of-bloom) confirmed that both bloom condition ( $F = 2.4942$ ,  $p = 0.003$ ) and patch ( $F = 5.5722$ ,  $p = 0.001$ ) were significant factors contributing to the difference in beta diversity observed in the prokaryotic communities in the whole community samples.

Unlike in the whole community, when considering the prokaryotes in the particle-attached fraction, the ALEX and MIX in-bloom samples clustered together away from the out-of-bloom and TRAN samples (Fig. 2D). The MARG in-bloom samples formed a third cluster separated from the rest of the prokaryotic communities (Fig. 2D). Therefore, prokaryotes associated with particles, and with the algal species themselves, responded differently than the overall prokaryotic community, especially during MIX and ALEX. Prokaryotic beta diversity in the particle-attached fraction was not homogeneously distributed, so no PERMANOVA test could be performed.

The blooming species of dinoflagellate, either *M. polykrikoides* or *A. monilatum*, dominated the microbiome for MIX and ALEX in-bloom samples in both the whole community and the particle-attached

fraction (Fig. 3). All other samples were dominated by prokaryotic taxa (Supplementary Figures 2 and 3). Members of the SAR11 clade Ia, though present in all whole community samples, were only present in the particle-attached fraction in ALEX in-bloom samples and one MIX in-bloom sample and were the dominant prokaryotic taxa in the ALEX in-bloom samples (Fig. 3). *Margalefidinium polykrikoides* was one of the dominating taxa in the MARG in-bloom samples in both the whole community and the particle-attached fraction. MARG in-bloom samples were co-dominated by the bacterial genus *Windogradskyella* (*Flavobacteriales*) and, in one case, the bacterial genus *Coraliomargarita* (*Opitutales*) in the whole community and by members of the dinoflagellate genus *Gymnodinium* in the particle-attached fraction (Fig. 3). *Windogradskyella* was the dominant prokaryote in the particle-attached fraction of MARG in-bloom samples, though the prokaryotic community made up a small percentage of the overall abundance of microbial organisms in those samples (Supplementary Figure 3). All out-of-bloom and TRAN in-bloom samples were dominated by *Cyanobium* and *Synechococcus* (*Synechococcales*) in both the whole community and in the particle-attached fraction (Fig. 3).

### 3.3. Particle-attached prokaryotes

Differences between observed patterns in prokaryotic beta diversity in the particle-attached fraction and the whole community, especially

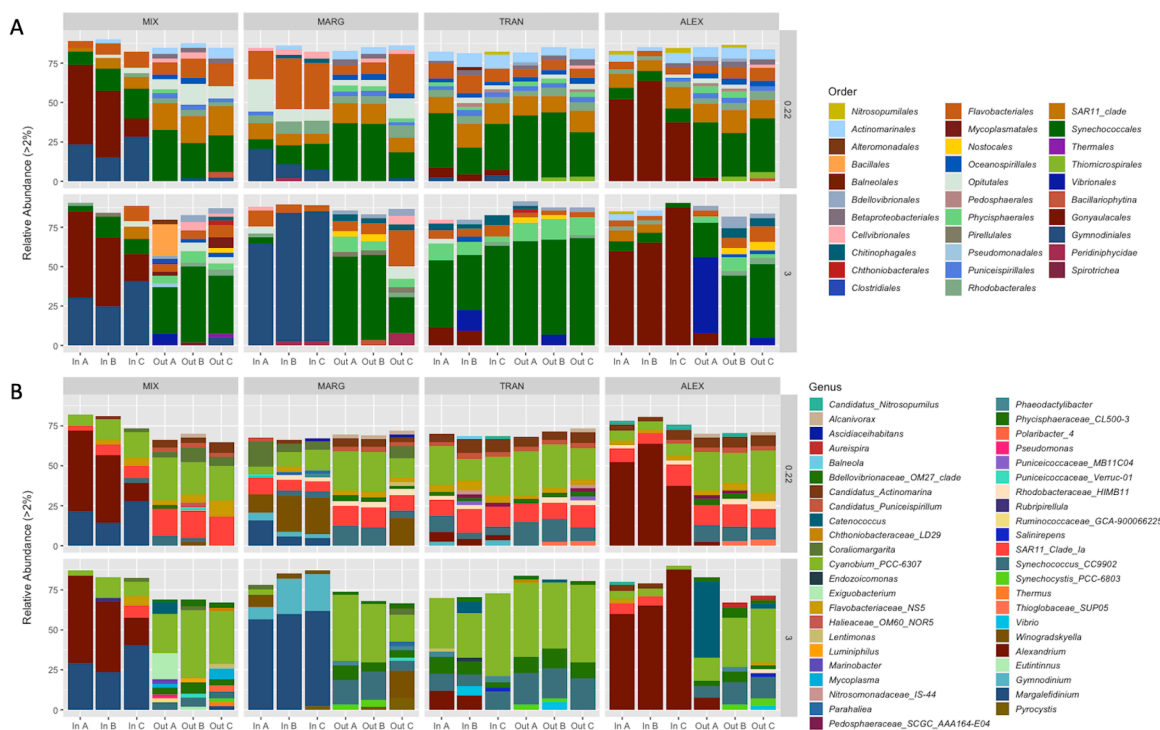


**Fig. 3.** Relative abundance of microbial orders (A) and genera (B) (>2%) present in whole community (0.22  $\mu$ m filter, top panels) and in the particle-attached fraction (3  $\mu$ m filter, bottom panels) samples collected from in-bloom (In) and out-of-bloom (Out) patches in each of the conditions during the 2017 bloom cycle (MIX: mix of *M. polykrikoides* and *A. monilatum*; MARG: bloom dominated by *M. polykrikoides*; TRAN: transition between blooms; ALEX: bloom dominated by *A. monilatum*).

during the *A. monilatum* bloom, show that the algae themselves, or particles or aggregates present in the water column, have a different microbiome structure than the overall microbiome in the estuarine water column. In order to identify the prokaryotic taxa with an increased relative abundance in the particle-attached fraction when high concentrations of *M. polykrikoides* or *A. monilatum* were present a heatmap, with triplicates averaged together, was used to visualize the relative abundance of prokaryotes associated with the different bloom conditions and patches (Fig. 4). One ALEX in-bloom particle-attached sample was highly dominated by *A. monilatum*, which made up almost 80% of the sequences. Because the prokaryotic sequences made up less than 25% of the total number of sequences in this sample it was removed from the heatmap analysis of the prokaryotic community.

The heatmap analysis showed that several prokaryotic taxa had increased relative abundance in the in-bloom samples during MIX, MARG, and ALEX, when high cell counts of the target dinoflagellate species were present. MARG in-bloom samples were associated with the bacterial genera *Winogradskyella* (Flavobacteriales) and *Coraliomargarita* (Opitutales), as seen in the whole community, though those genera were not present in ALEX in-bloom samples in the particle-attached fraction (Fig. 4). ALEX in-bloom samples were associated with a unique group of genera that were only present in a high abundance in the particle-attached fraction in the ALEX in-bloom and, to a lesser degree, the MIX in-bloom samples where *A. monilatum* cells were also present. These genera include *Candidatus Nitrosopumilus*, *Candidatus Actinomarina*, SAR11 Clade Ia, *Candidatus Bealeia*, and *Rhodobacteraceae HIMB11* and appear to be strongly, positively associated with *A. monilatum*, though further research will need to be performed to confirm the nature of the association (Fig. 4).

#### 3.4. Correlations between microbial taxa and environmental characteristics

Spearman correlations, combining in- and out-of-bloom samples,

were used to determine which of the top 25 most abundant genera, those with greater than 10% relative abundance in the whole community, were associated with the concentrations of DOC, DIC, DON,  $\text{NO}_x$ , and  $\text{NH}_4^+$  during the different bloom conditions (Fig. 5). *Margalefidiinum*, *Gymnodinium*, and *Alexandrium* were the only genera to have a negative correlation with DIC during the MIX bloom week. Instead, those genera were positively correlated with DOC, DON, and inorganic nitrogen species (Fig. 5). Prokaryotic genera were positively correlated with DIC, especially during the MIX and ALEX bloom weeks. Many heterotrophic genera, including *Winogradskyella*, *Puniceicoccaceae Verruc\_01*, *Flavobacteriaceae* marine group NS5, and *Coraliomargarita*, were positively correlated with DOC and DON during MARG and TRAN weeks, though many of those same genera were negatively correlated with DOC and DON during the MIX bloom condition (Fig. 5). Two genera of ammonium oxidizing prokaryotes, *Nitrosomonadaceae IS44* and *Candidatus Nitrosopumilus*, were positively correlated with  $\text{NH}_4^+$  and  $\text{NO}_x$  during the TRAN bloom condition, though were negatively, and in the case of *Nitrosomonadaceae IS44* significantly, correlated with  $\text{NH}_4^+$  and  $\text{NO}_x$  during the MIX bloom condition (Fig. 5).

## 4. Discussion

The blooms dominated by *M. polykrikoides* and *A. monilatum* changed the overall microbiome present in the surface water of the York River Estuary. Four distinct microbiome compositions were observed during the 2017 York River HAB cycle, one when no large dinoflagellate bloom was present (i.e., during TRAN and in the out-of-bloom samples), one when *M. polykrikoides* was dominant, one when *A. monilatum* was dominant, and one when the bloom was dominated by a mix of *M. polykrikoides* and *A. monilatum*. Blooms of the two different species led to a switch from prokaryotic dominated primary producers, primarily *Cyanobium* and *Synechococcus* (Synechococcales), to eukaryotic primary producers dominated by dinoflagellate species in the in-bloom samples. A decrease in *Cyanobacteria* during *M. polykrikoides* blooms has

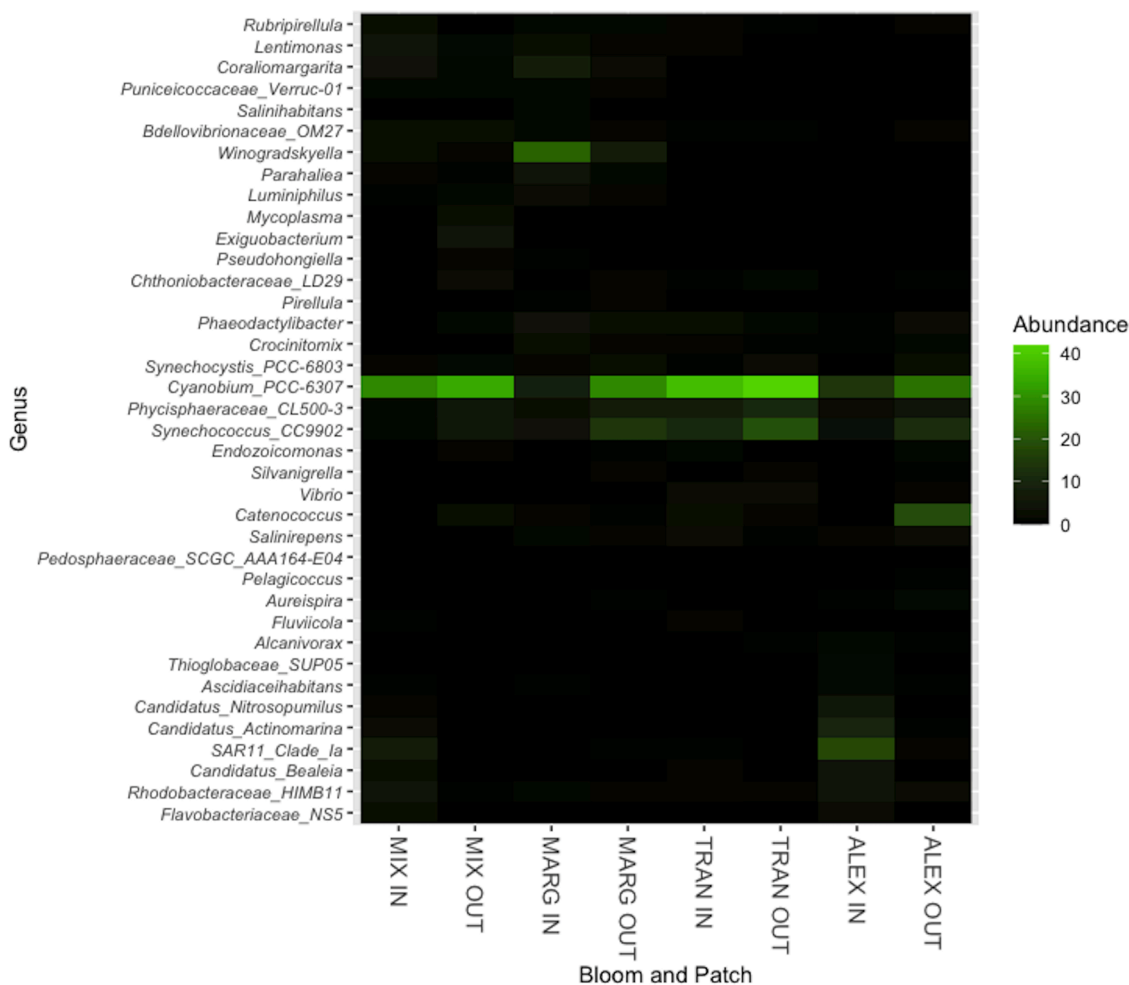


**Fig. 4.** A heatmap of the relative abundance of prokaryotic genera (>2%) in the particle-attached fraction (3  $\mu\text{m}$  filter). Taxa abundances for each bloom and patch are averages of the three replicates for each in-bloom and out-of-bloom condition (MIX: mix of *M. polykrikoides* and *A. monilatum*; MARG: bloom dominated by *M. polykrikoides*; TRAN: transition between blooms; ALEX: bloom dominated by *A. monilatum*).

been seen previously in other estuaries (Koch et al., 2014). *Cyanobium* and *Synechococcus* were also present in the particle-attached fraction despite being too small for the 3  $\mu\text{m}$  filter to capture if they were free-living single-cells, though their abundance decreased in the particle-attached fraction in MARG and ALEX in-bloom samples. *Cyanobacteria* have been observed previously in particle-attached fractions in association with *M. polykrikoides* blooms which could imply attachment of various *Cyanobacteria* to the algal cells, the consumption of different *Cyanobacteria* by the mixotrophic dinoflagellate species, or conglomeration of the *Cyanobacteria* with each other (Hattenrath-Lehmann et al., 2019; Jeong et al., 2010). All in-bloom samples during bloom weeks (excluding TRAN) also had a decreased alpha diversity, a trend that has been previously reported in studies of HAB associated microbiomes (Hattenrath-Lehmann et al., 2019). However, blooms of *M. polykrikoides* and *A. monilatum*, and the mix of the two algal species, resulted in different microbiomes and appeared to drive community changes in different ways.

Prokaryotic communities in the MARG in-bloom samples were different from out-of-bloom samples as well as from the in-bloom samples during MIX and ALEX in both the whole community and the particle-attached fraction. The changes in prokaryotic communities during the MARG bloom appear to be linked to DOC and DON produced by *M. polykrikoides*. During MIX and MARG, the highest concentrations of DOC and DON were observed in the in-bloom samples, despite having lower concentrations of algae than ALEX in-bloom samples. In addition, bacterial taxa with increased abundances in the whole community

during MARG, the genera *Winogradskyella* and *Coraliomargarita*, had positive correlations with DOC and DON during MARG and TRAN. Both genera were associated with in-bloom samples during MARG in the particle-attached fraction. The increase in taxa belonging to the heterotrophic order *Flavobacteriales* during blooms of *M. polykrikoides* and other harmful algal species has been seen previously (Hattenrath-Lehmann et al., 2019; Hattenrath-Lehmann and Gobler, 2017; Koch et al., 2014) and *Winogradskyella* has been found to be associated with non-harmful and harmful phytoplankton blooms, including those of *M. polykrikoides*, in the past (Alejandro-Colomo et al., 2021; Hattenrath-Lehmann et al., 2019). The genus *Coraliomargarita* has also been previously observed to have positive associations with *M. polykrikoides* blooms (Hattenrath-Lehmann et al., 2019).

Heterotrophic bacteria remineralize the excess DOC and DON produced by the large concentration of algae (Azam et al., 1983), and heterotrophic bacteria, especially those belonging to the orders *Flavobacteriales* and *Rhodobacteriales* have often been observed to increase in response to algal blooms (Buchan et al., 2014). The higher concentration of DOC and DON in in-bloom samples when *M. polykrikoides* was present, despite the lower cell count in the *M. polykrikoides* bloom, combined with the increase in heterotrophic bacteria in MIX and MARG in-bloom samples, implies that *M. polykrikoides* releases more DOC and DON than *A. monilatum*. *M. polykrikoides* is an athenated dinoflagellate and lyses more easily than the thecated *A. monilatum* (data not shown), likely leading to more cell lysis in the water column and increasing the release of DOC and DON into surface water. Another

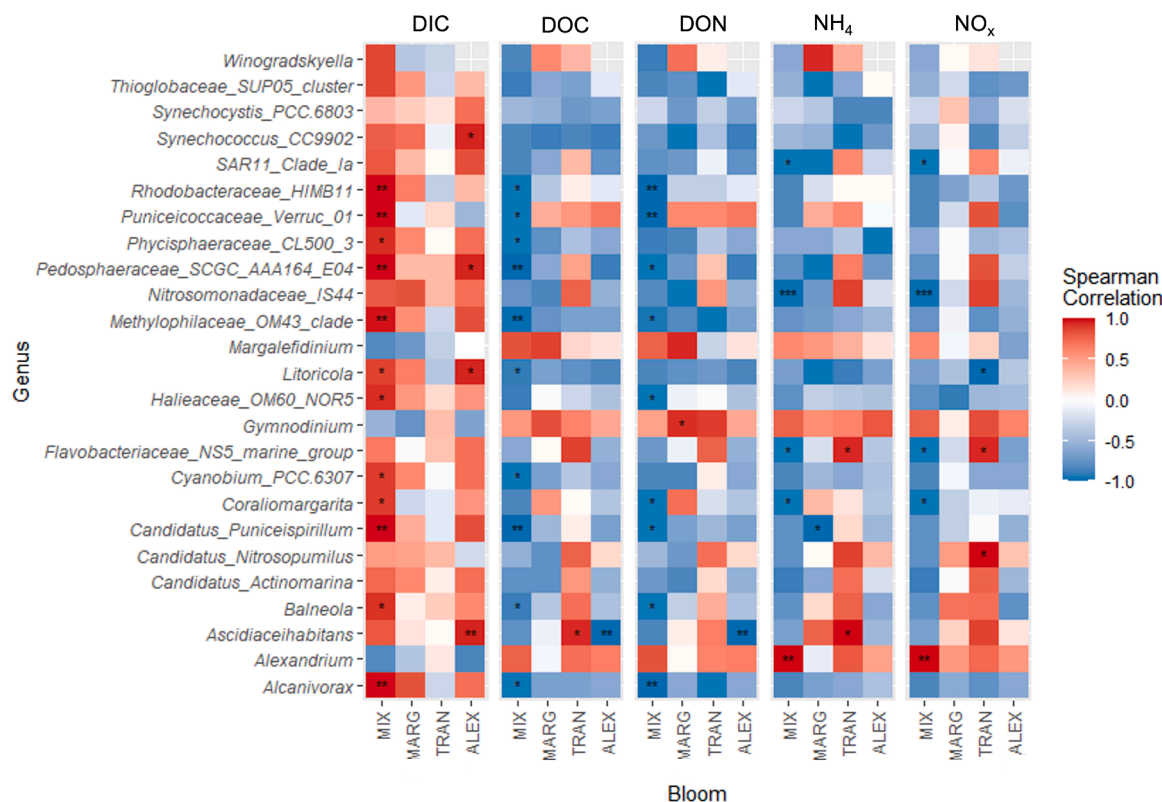


**Fig. 5.** Spearman correlation heatmap representing the correlation between the relative abundance of the top 25 microbial genera (all >10% relative abundance) and concentrations of dissolved inorganic carbon (DIC), dissolved organic carbon (DOC), dissolved organic nitrogen (DON), ammonium (NH<sub>4</sub>), and nitrate/nitrite (NO<sub>x</sub>). Six samples (3 in-bloom, 3 out-of-bloom) were averaged together for each bloom condition (MIX: mix of *M. polykrikoides* and *A. monilatum*; MARG: bloom dominated by *M. polykrikoides*; TRAN: transition between blooms; ALEX: bloom dominated by *A. monilatum*). Stars represent significance using adjusted p-values from multiple comparisons of spearman correlations (\* is  $p < 0.05$ , \*\* is  $p < 0.01$ ).

explanation for the lower concentrations of DOC and DON during ALEX is that the *A. monilatum* cells could be taking up and using the DOC and DON produced by *M. polykrikoides* and other cells. Many heterotrophic bacteria likely used the algal produced DOC and DON as carbon and nitrogen sources for growth and survival as has been seen in other blooms, including previous *A. monilatum* blooms in the York River (Buchan et al., 2014; Han et al., 2021; Killberg-Thoreson et al., 2021). Further studies should be conducted to determine the impact of algal produced DOC and DON on York River dinoflagellate blooms.

Unlike the *M. polykrikoides* bloom which altered the prokaryotic portion of the York River microbiome in both the whole community and the particle-attached fraction, the *A. monilatum* bloom did not impact the prokaryotes in the whole community, but instead had a strong impact on the prokaryotic community in the particle-attached fraction. This is the first report of microbiomes present in an *A. monilatum* bloom, though previous studies on other *Alexandrium* species including *A. minutum*, *A. tamarensis*, and *A. catenella*, have been performed using a variety of molecular tools (Garcés et al., 2007). The previous studies have seen increases in the relative abundance of prokaryotic taxa in the orders *Rhodobacterales*, SAR11, *Altermonadaceae*, *Oceanospirillales*, and *Flavobacteriales*, specifically the NS5 marine group and *Owenweeksia*, during *Alexandrium* sp. blooms (Garcés et al., 2007; Hattenrath-Lehmann et al., 2019; Hattenrath-Lehmann and Gobler, 2017; Jasti et al., 2005). Since ALEX did not have a different prokaryotic community structure in the whole community, there was not a large overall increase of any heterotrophic prokaryotes during the *A. monilatum* bloom. Instead, *A. monilatum* appears to selectively drive prokaryotic associations in the particle-attached fraction of the microbiomes, with both the MIX in-bloom and ALEX in-bloom samples grouping together in the particle-attached fraction despite clustering separately in the whole community.

There were several specific positive associations seen in the particle-attached fraction that were only present for ALEX and, to a lesser degree, MIX in-bloom samples where *A. monilatum* was present. Associations of other species in the *Alexandrium* genus with *Alphaproteobacteria* in general and the SAR11 clade in particular have been previously reported (Garcés et al., 2007; Hattenrath-Lehmann and Gobler, 2017; Jasti et al., 2005; Shin et al., 2018) so the association of SAR11 Clade Ia with *A. monilatum* is no surprise. Unlike previous studies, no evidence of an association between *A. monilatum* and any *Flavobacteriales* taxa was found. Associations between *Alexandrium* species and the ammonium oxidizing archaea *Candidatus Nitrosopumilus* have not been previously reported, though this could be due to the methods used in previous studies, many of which looked for specific bacterial lineages predicted to be associated with algal blooms (Garcés et al., 2007). The relative abundance of *Candidatus Nitrosopumilus* was correlated with NH<sub>4</sub><sup>+</sup> and NO<sub>x</sub> concentrations during TRAN and ALEX bloom conditions. *Candidatus Nitrosopumilus* could have played an important role in regulating the speciation of inorganic nitrogen and the availability of NO<sub>x</sub> and NH<sub>4</sub><sup>+</sup>, while the *A. monilatum* bloom was developing, though more research would need to be performed to determine if this is the case. The close association between *A. monilatum* and the above-mentioned taxa could indicate that these prokaryotes perform important roles in *A. monilatum*'s lifecycle and physiology or that these prokaryotes are better able to use extracellular material produced by *A. monilatum*; both possibilities require further research to better understand *A. monilatum* and its bloom forming tendencies but were outside the scope of this study.

Both *M. polykrikoides* and *A. monilatum* are harmful algal species due to their toxic effect on other organisms (Anderson et al., 2012; Harding et al., 2009; Kudela and Gobler, 2012; May et al., 2010; Mulholland et al., 2009). While *A. monilatum* has a known toxin (goniodomin A)

(Espiña et al., 2016), which has been observed in the York River during previous blooms of *A. monilatum* (Harris et al., 2020), a toxin has not been identified for *M. polykrikoides*. The observed changes in microbiome associated with blooms of these species could be due, in part, to their toxic nature. The selective nature of *A. monilatum*, in regard to its closely associated group of prokaryotes, could be due to the ability of those specific prokaryotes to survive goniiodomin A exposure while other prokaryotes are harmed or killed by exposure to *A. monilatum*. This study, however, was not designed to investigate the impact of algal toxins on microbiomes, but instead to investigate the overall impact of the blooms of these organisms on the estuarine microbiome. Therefore, further research would need to be performed to determine if the harmful or toxic nature of *M. polykrikoides* or *A. monilatum* has a distinct effect on the microbiome.

When considering the overall impact of HABs on estuarine systems, it is not only the effect of toxins produced by the HABs that can impact the microbiome, but also the effect of the localized increase in primary production. The introduction of high concentrations of organic matter to the estuarine system is expected to encourage the growth of heterotrophic bacteria (Azam et al., 1983; Buchan et al., 2014). This was indeed the case with the bloom dominated by *M. polykrikoides*, but not for the bloom dominated by *A. monilatum*. The disparity in microbiome responses between these different species appears to be linked to the amount of DOC and DON produced by the species and the responses of prokaryotes to that algal produced DOC and DON. Hypoxia is often linked to the production of biomass and organic matter from algal blooms as the heterotrophic bacteria remineralize the organic matter and use up the available oxygen in the estuarine water column (Paerl et al., 1998). Since the *M. polykrikoides* bloom produced a greater amount of DOC and DON, despite having a lower cell count, and was closely tied to the increase in heterotrophic bacteria, this indicates that blooms of this species are more likely to impact overall estuarine carbon cycling and may have a greater likelihood of leading to hypoxic or anoxic events than blooms of *A. monilatum*. Furthermore, this study shows that blooms of different algal species can affect the microbiome of a system in different ways, likely changing the impact of these blooms on the estuarine carbon and nitrogen cycling processes associated with the estuarine microbiome.

## 5. Conclusions

This study was not only the first to examine the microbiome of blooms dominated by the harmful alga *A. monilatum*, but also one of the few studies to identify changes in estuarine microbiomes associated with consecutive algal blooms. By examining both algal blooms, and the transition period between the blooms, this study was able to observe differential changes in the microbiomes between the two blooms and observe the changes in prokaryotic community response to the presence or absence of blooming organisms.

Overall, the two blooms of dinoflagellates led to changes in the estuarine microbiome, impacting both eukaryotic and prokaryotic microorganisms. The bloom dominated by *M. polykrikoides* was characterized by increased DOC and DON concentrations and a large increase in the relative abundance of heterotrophic prokaryotes, specifically *Winogradskyella*. The larger bloom dominated by *A. monilatum*, on the other hand, had almost no impact on the overall prokaryotic community but instead was closely associated group of prokaryotes in the particle-attached fraction including *Candidatus Nitrosopumilus*, *Candidatus Actinomarina*, SAR11 Clade Ia, *Candidatus Bealeia*, and *Rhodobacteraeae* sp. HIMB11. This study illustrates the impact large algal blooms can have on the estuarine ecosystem, while emphasizing the need to examine blooms of different algal species individually and to consider the impact of changing estuarine biogeochemistry related to large algal blooms on the overall microbiome and biogeochemical cycling of the estuarine water column.

## Declaration of Competing Interest

The authors declare that they have no known competing financial interests or personal relationships that could have appeared to influence the work reported in this paper.

## Acknowledgements

We would like to thank Hunter Walker, Stephanie Wilson, Shanna Williamson, Mark Brush, Gail Scott, Alanna Macintyre, Clara Robison, and William Jones for their assistance in the lab and field. Funding for this study was provided by the National Science Foundation [OCE 1737258] and the National Oceanographic and Atmospheric Administration [ECOHAB NA17NOS4780182]. This is Virginia Institute of Marine Science, William and Mary contribution 4083 and ECOHAB publication ECO1016.

## Supplementary materials

Supplementary material associated with this article can be found, in the online version, at [doi:10.1016/j.hal.2022.102216](https://doi.org/10.1016/j.hal.2022.102216).

## References

Alejandre-Colomo, C., Francis, B., Viver, T., Harder, J., Fuchs, B.M., Rossello-Mora, R., Amann, R., 2021. Cultivable *Winogradskyella* species are genetically distinct from the sympatric abundant candidate species. *ISME Commun.* 1 <https://doi.org/10.1038/s43705-021-00052-w>.

Anderson, D.M., Alpermann, T.J., Cembella, A.D., Collos, Y., Masseret, E., Montresor, M., 2012. The globally distributed genus *Alexandrium*: multifaceted roles in marine ecosystems and impacts on human health. *Harmful Algae* 14, 10–35. <https://doi.org/10.1016/j.hal.2011.10.012>.

Anderson, I.C., McGlathery, K.J., Tyler, A.C., 2003. Microbial mediation of “reactive” nitrogen transformations in a temperate lagoon. *Mar. Ecol. Prog. Ser.* 246, 73–84. <https://doi.org/10.3354/meps246073>.

Azam, F., Fenchel, T., Field, J., Gray, J., Meyer-Reil, L., Thingstad, F., 1983. The ecological role of water-column microbes in the sea. *Mar. Ecol. Prog. Ser.* 10, 257–263. <https://doi.org/10.3354/meps010257>.

Balech, E., 1995. The Genus *Alexandrium* Halim (Dinoflagellata). *Sherkin Island Marine Station, Cork, Ireland*.

Buchan, A., LeCleir, G.R., Gulvik, C.A., González, J.M., 2014. Master recyclers: features and functions of bacteria associated with phytoplankton blooms. *Nat. Rev. Microbiol.* 12, 686–698. <https://doi.org/10.1038/nrmicro3326>.

Callahan, B.J., McMurdie, P.J., Rosen, M.J., Han, A.W., Johnson, A.J.A., Holmes, S.P., 2016. DADA2: high resolution sample inference from Illumina amplicon data. *Nat. Methods* 13, 581–583. <https://doi.org/10.1038/nmeth.3869.DADA2>.

Croft, M.T., Lawrence, A.D., Raux-Deery, E., Warren, M.J., Smith, A.G., 2005. Algae acquire vitamin B12 through a symbiotic relationship with bacteria. *Nature* 438, 90–93. <https://doi.org/10.1038/nature04056>.

Doucette, G., 1995. Interactions between bacteria and harmful algae: a review. *Nat. Toxins* 3, 65–74.

Espiña, B., Cagide, E., Louzao, M.C., Vilariño, N., Vieytes, M.R., Takeda, Y., Sasaki, M., Botana, L.M., 2016. Cytotoxicity of goniiodomin A and B in non contractile cells. *Toxicol. Lett.* 250–251. <https://doi.org/10.1016/j.toxlet.2016.04.001>, 10–20.

Garcés, E., Vila, M., Reñé, A., Alonso-Sáez, L., Anglès, S., Lugliè, A., Masó, M., Gasol, J. M., 2007. Natural bacterioplankton assemblage composition during blooms of *Alexandrium* spp. (Dinophyceae) in NW Mediterranean coastal waters. *Aquat. Microb. Ecol.* 46, 55–70. <https://doi.org/10.3354/ame046055>.

Gobler, C.J., Burson, A., Koch, F., Tang, Y., Mulholland, M.R., 2012. The role of nitrogenous nutrients in the occurrence of harmful algal blooms caused by *Cochlodinium polykrikoides* in New York estuaries (USA). *Harmful Algae* 17, 64–74. <https://doi.org/10.1016/j.hal.2012.03.001>.

Gómez, F., Richlen, M.L., Anderson, D.M., 2017. Molecular characterization and morphology of *Cochlodinium strangulatum*, the type species of *Cochlodinium*, and *Margalefidinium* gen. nov. for *C. polykrikoides* and allied species (Gymnodiniales, Dinophyceae). *Harmful Algae* 63, 32–44. <https://doi.org/10.1016/j.hal.2017.01.008>.

Han, Y., Jiao, N., Zhang, Y., Zhang, F., He, C., Liang, X., Cai, R., Shi, Q., Tang, K., 2021. Opportunistic bacteria with reduced genomes are effective competitors for organic nitrogen compounds in coastal dinoflagellate blooms. *Microbiome* 9. <https://doi.org/10.1186/s40168-021-01022-z>.

Harding, J.M., Mann, R., Moeller, P., Hsia, M.S., 2009. Mortality of the veined rapa whelk, *Rapana venosa*, in relation to a bloom of *Alexandrium monilatum* in the York River, United States. *J. Shellfish Res.* 28, 363–367. <https://doi.org/10.2983/035.028.0219>.

Harris, C.M., Reece, K.S., Stec, D.F., Scott, G.P., Jones, W.M., Hobbs, P.L.M., Harris, T.M., 2020. The toxin goniiodomin, produced by *Alexandrium* spp., is identical to goniiodomin A. *Harmful Algae* 92, 101707. <https://doi.org/10.1016/j.hal.2019.101707>.

Hattenrath-Lehmann, T.K., Gobler, C.J., 2017. Identification of unique microbiomes associated with harmful algal blooms caused by *Alexandrium fundyense* and *Dinophysis acuminata*. *Harmful Algae* 68, 17–30. <https://doi.org/10.1016/j.hal.2017.07.003>.

Hattenrath-Lehmann, T.K., Jankowiak, J., Koch, F., Gobler, C.J., 2019. Prokaryotic and eukaryotic microbiomes associated with blooms of the ichthyotoxic dinoflagellate *Cochlodinium* (Margalefidinum) polykrikoides in New York, USA, estuaries. *PLoS One* 14, 1–26. <https://doi.org/10.1371/journal.pone.0223067>.

Heisler, J., Glibert, P.M., Burkholder, J.M., Anderson, D.M., Cochlan, W., Dennison, W.C., Dortch, Q., Gobler, C.J., Heil, C.A., Humphries, E., Lewitus, A., Magnien, R., Marshall, H.G., Sellner, K., Stockwell, D.A., Stoecker, D.K., Sudleson, M., 2008. Eutrophication and harmful algal blooms: a scientific consensus. *Harmful Algae* 8, 3–13. <https://doi.org/10.1016/j.hal.2008.08.006>.

Hsia, M.H., Morton, S.L., Smith, L.L., Beauchesne, K.R., Huncik, K.M., Moeller, P.D.R., 2006. Production of goniiodomin by the planktonic, chain-forming dinoflagellate *Alexandrium monilatum* (Howell) Balech isolated from the Gulf Coast of the United States. *Harmful Algae* 5, 290–299. <https://doi.org/10.1016/j.hal.2005.08.004>.

Jasti, S., Sieracki, M.E., Poulton, N.J., Giewat, M.W., Rooney-Varga, J.N., 2005. Phylogenetic diversity and specificity of bacteria closely associated with *Alexandrium* spp. and other phytoplankton. *Appl. Environ. Microbiol.* 71, 3483–3494. <https://doi.org/10.1128/AEM.71.7.3483-3494.2005>.

Jeong, H.J., Yoo, Y.du, Kim, J.S., Seong, K.A., Kang, N.S., Kim, T.H., 2010. Growth, feeding and ecological roles of the mixotrophic and heterotrophic dinoflagellates in marine planktonic food webs. *Ocean Sci. J.* 45, 65–91. <https://doi.org/10.1007/s12601-010-0007-2>.

Killberg-Thoreson, L., Baer, S.E., Sipler, R.E., Reay, W.G., Roberts, Q.N., Bronk, D.A., 2021. Seasonal nitrogen uptake dynamics and harmful algal blooms in the York River, Virginia. *Estuaries Coasts* 44, 750–768. <https://doi.org/10.1007/s12237-020-00802-4> [Published].

Koch, F., Burson, A., Tang, Y.Z., Collier, J.L., Fisher, N.S., Sañudo-Wilhelmy, S., Gobler, C.J., 2014. Alteration of plankton communities and biogeochemical cycles by harmful *Cochlodinium* polykrikoides (Dinophyceae) blooms. *Harmful Algae* 33, 41–54. <https://doi.org/10.1016/j.hal.2014.01.003>.

Kodama, M., Doucette, G.J., Green, D.H., Graneli, E., Turner, J.T., 2006. Relationships between bacteria and harmful algae. *Ecology of Harmful Algae*. Springer, New York, pp. 243–255.

Koroleff, F., Grasshoff, K., Ehrhardt, M., Kremling, K., 1983. Total and organic nitrogen. *Methods of Seawater Analysis*. Verlag-Chemie, Weinheim, pp. 162–169.

Kudela, R.M., Gobler, C.J., 2012. Harmful dinoflagellate blooms caused by *Cochlodinium* sp.: global expansion and ecological strategies facilitating bloom formation. *Harmful Algae* 14, 71–86. <https://doi.org/10.1016/j.hal.2011.10.015>.

Lee, C.K., Park, T.G., Park, Y.T., Lim, W.A., 2013. Monitoring and trends in harmful algal blooms and red tides in Korean coastal waters, with emphasis on *Cochlodinium* polykrikoides. *Harmful Algae* 30, 3–14. <https://doi.org/10.1016/j.hal.2013.10.002>.

Liao, N., 2001. Determination of ammonia in brackish or seawater by flow injection analysis. *QuikChem Method*, 31-107-06-1-B.

Marshall, H.G., Egerton, T.A., 2009. Phytoplankton blooms: their occurrence and composition within Virginia's tidal tributaries. *Virginia J. Sci.* 60, 149–164.

May, S.P., Burkholder, J.A.M., Shumway, S.E., Hégaret, H., Wikfors, G.H., Frank, D., 2010. Effects of the toxic dinoflagellate *Alexandrium monilatum* on survival, grazing and behavioral response of three ecologically important bivalve molluscs. *Harmful Algae* 9, 281–293. <https://doi.org/10.1016/j.hal.2009.11.005>.

McMurdie, P.J., Holmes, S., 2013. Phyloseq: an R package for reproducible interactive analysis and graphics of microbiome census data. *PLoS One* 8. <https://doi.org/10.1371/journal.pone.0061217>.

Mulholland, M.R., Morse, R.E., Boneillo, G.E., Bernhardt, P.W., Filippino, K.C., Procise, L.A., Blanco-Garcia, J.L., Marshall, H.G., Egerton, T.A., Hunley, W.S., Moore, K.A., Berry, D.L., Gobler, C.J., 2009. Understanding causes and impacts of the dinoflagellate, *Cochlodinium polykrikoides*, blooms in the Chesapeake Bay. *Estuaries Coasts* 32, 734–747. <https://doi.org/10.1007/s12237-009-9169-5>.

Neubauer, S.C., Anderson, I.C., 2003. Transport of dissolved inorganic carbon from a tidal freshwater marsh to the York River estuary. *Limnol. Oceanogr.* 48, 299–307.

Oksanen, J., Blanchet, F.G., Friendly, M., Kindt, R., Legendre, P., McGlinn, D., Minchin, P.R., O'Hara, R.B., Simpson, G.L., Solymos, P., Stevens, M.H.H., Szoecs, E., Wagner, H., 2018. Vegan: community ecology package.

Pael, H.W., Pinckney, J.L., Fear, J.M., Peierls, B.L., 1998. Ecosystem responses to internal and watershed organic matter loading: consequences for hypoxia in the eutrophying Neuse River Estuary. *Mar. Ecol. Progress Series* 166, 17–25.

Parada, A.E., Needham, D.M., Fuhrman, J.A., 2016. Every base matters: assessing small subunit rRNA primers for marine microbiomes with mock communities, time series and global field samples. *Environ. Microbiol.* 18, 1403–1414. <https://doi.org/10.1111/1462-2920.13023>.

R Core Team, 2018. R: a language and environment for statistical computing.

Reay, W.G., 2009. Water quality within the York River estuary. *J. Coastal Res.* 10057, 23–39. <https://doi.org/10.2112/1551-5036-57.sp1.23>.

Sellner, K.G., Doucette, G.J., Kirkpatrick, G.J., 2003. Harmful algal blooms: causes, impacts and detection. *J. Ind. Microbiol. Biotechnol.* 30, 383–406. <https://doi.org/10.1007/s10295-003-0074-9>.

Sharp, J.H., Beauregard, A.Y., Burdige, D., Cauwet, G., Curless, S.E., Lauck, R., Nagel, K., Ogawa, H., Parker, A.E., Prim, O., Pujo-Pay, M., Savidge, W.B., Seitzinger, S., Spyres, G., Styles, R., 2004. A direct instrument comparison for measurement of total dissolved nitrogen in seawater. *Mar. Chem.* 84, 181–193. <https://doi.org/10.1016/j.marchem.2003.07.003>.

Shin, H., Lee, E., Shin, J., Ko, S.R., Oh, H.S., Ahn, C.Y., Oh, H.M., Cho, B.K., Cho, S., 2018. Elucidation of the bacterial communities associated with the harmful microalgae *Alexandrium tamarense* and *Cochlodinium polykrikoides* using nanopore sequencing. *Sci. Rep.* 8, 4–11. <https://doi.org/10.1038/s41598-018-23634-6>.

Smith, P., Bogren, K., 2001. Determination of nitrate and/or nitrite in brackish or seawater by flow injection analysis colorimetry. *QuikChem Method*, 31-107-04-1-E.

Smith, S., 2019. phylosmith: an R-package for reproducible and efficient microbiome analysis with phyloseq-objects. *J. Open Source Software* 4, 1442. <https://doi.org/10.21105/joss.01442>.

Ssekagiri, A., Sloan, W.T., Ijaz, U.Z., 2017. microbiomeSeq: an R package for analysis of microbial communities in an environmental context. In: ISCB Africa ASBCB Conference. <https://doi.org/10.13140/RG.2.2.17108.71047>.

Stoecker, D.K., Hansen, P.J., Caron, D.A., Mitra, A., 2017. Mixotrophy in the marine plankton. *Annu. Rev. Mar. Sci.* 9, 311–335. <https://doi.org/10.1146/annurev-marine-010816-060617>.

Tang, Y.Z., Gobler, C.J., 2009. *Cochlodinium polykrikoides* blooms and clonal isolates from the northwest Atlantic coast cause rapid mortality in larvae of multiple bivalve species. *Mar. Biol.* 156, 2601–2611. <https://doi.org/10.1007/s00227-009-1285-z>.

Vandersea, M.W., Kibler, S.R., van Sant, S.B., Tester, P.A., Sullivan, K., Eckert, G., Cammarata, C., Reece, K., Scott, G., Place, A., Holdierd, K., Hondolero, D., Litaker, R.W., 2017. qPCR assays for *Alexandrium fundyense* and *A. ostenfeldii* (Dinophyceae) identified from Alaskan waters and a review of species-specific *Alexandrium* molecular assays. *Phycologia* 56, 303–320. <https://doi.org/10.2216/16-41.1.qPCR>.

Wickham, H., 2005. ggplot2: create elegant data visualisations using the grammar of graphics.

Wolny, J.L., Tomlinson, M.C., Schollaert Uz, S., Egerton, T.A., McKay, J.R., Meredith, A., Reece, K.S., Scott, G.P., Stumpf, R.P., 2020. Current and future remote sensing of harmful algal blooms in the Chesapeake Bay to support the shellfish industry. *Front. Mar. Sci.* 7, 1–16. <https://doi.org/10.3389/fmars.2020.00337>.

Yilmaz, P., Parfrey, L.W., Yarza, P., Gerken, J., Pruesse, E., Quast, C., Schweer, T., Peplies, J., Ludwig, W., Glöckner, F.O., 2014. The SILVA and “all-species living tree project (LTP)” taxonomic frameworks. *Nucleic Acids Res.* 42, 643–648. <https://doi.org/10.1093/nar/gkt1209>.